Shot Noise in Digital Holography

Fadwa Joud, Frédéric Verpillat, Michael Atlan, Pierre-André Taillard, Michel Gross

Shot Noise in Digital Holography

Fadwa Joud, Frédéric Verpillat, Michael Atlan, Pierre-André Taillard, and Michel Gross

Abstract We discuss on noise in heterodyne holography in an off-axis configuration. We show that, for a weak signal, the noise is dominated by the shot noise on the reference beam. This noise corresponds to an equivalent noise on the signal beam of 1 photo electron per pixel, for the whole sequence of images used to build the digital hologram.

1 Introduction

Demonstrated by Gabor [1] in the early 50's, the purpose of holography is to record, on a 2D detector, the phase and the amplitude of the radiation field scattered by an object under coherent illumination. The photographic film used in conventional holography is replaced by a 2D electronic detection in digital holography [2] en-

Fadwa Joud
Laboratoire Kastler Brossel École Normale Supérieure , UMR 8552 , UPMC, CNRS 24 rue Lhomond , 75231 Paris Cedex 05. e-mail: joud@lkb.ens.fr

Frédéric Verpillat
Laboratoire Kastler Brossel École Normale Supérieure , UMR 8552 , UPMC, CNRS 24 rue Lhomond , 75231 Paris Cedex 05, e-mail: verpillat@lkb.ens.fr

Michael Atlan
Fondation Pierre-Gilles de Gennes, Institut Langevin: UMR 7587 CNRS, U 979 INSERM, ESPCI ParisTech, Université Paris 6, Université Paris 7, 10 rue Vauquelin, 75 231 Paris Cedex 05, France.e-mail: atlan@optique.espci.fr

Pierre-André Taillard
Conservatoire de musique neuchâtelois; Avenue Léopold-Robert 34 ; 2300 La Chaux-de-Fonds ; Suisse.e-mail: taillard@hispeed.ch

Michel Gross
Laboratoire Kastler Brossel École Normale Supérieure , UMR 8552 , UPMC, CNRS 24 rue Lhomond , 75231 Paris Cedex 05. e-mail: gross@lkb.ens.fr

abling quantitative numerical analysis. Digital holography has been waiting for the recent development of computer and video technology to be experimentally demonstrated [3]. The main advantage of digital holography is that, contrary to holography with photographic plates [1], the holograms are recorded by a CCD, and the image is digitally reconstructed by a computer, avoiding photographic processing [4].

Off-axis holography [5] is the oldest configuration adapted to digital holography [6, 3, 7]. In off-axis digital holography, as well as in photographic plate holography, the reference or local oscillator (LO) beam is angularly tilted with respect to the object observation axis. It is then possible to record, with a single hologram, the two quadratures of the object's complex field. However, the object field of view is reduced, since one must avoid the overlapping of the image with the conjugate image alias [8]. In Phase-shifting digital holography, which has been introduced later [9], several images are recorded with different LO beam phases. It is then possible to obtain the two quadratures of the object field in an in-line configuration even though the conjugate image alias and the true image overlap, because aliases can be removed by taking image differences.

We have developed an alternative phase-shifting digital holography technique, called heterodyne holography, that uses a frequency shift of the reference beam to continuously shift the phase of the recorded interference pattern [10]. One of the advantages of this technique is its ability to provide accurate phase shifts that allow to suppress twin images aliases [11]. This greatly simplifies holographic data handling, and improves sensitivity. Moreover, it is possible to perform holographic detection at a frequency different from illumination. One can for example detect "tagged photons" [12, 13] in ultrasound-modulated optical imaging [14]. One can also also image vibrating objects at the frequencies corresponding to vibration sidebands [15, 16]. To the end, it is possible to perform Laser Doppler imaging [17] within microvessels [18, 19, 20].

More generally, our setup can be viewed as a multipixel heterodyne detector that is able of recording the complex amplitude of the signal electromagnetic field $\mathscr{E}$ onto all pixels of the CCD camera in parallel. We get the map of the field over the array detector (i.e. $\mathscr{E}(x,y)$ where x and y are the pixels coordinates). Since the field is measured on all pixels at the same time, the relative phase that is measured for different locations (x,y) is meaningful. This means that the field map $\mathscr{E}(x,y)$ is a hologram that can be used to reconstruct the field $\mathscr{E}$ in any location, in particular in the object plane.

In the present paper we will discuss on noise in digital holography, and we will try to determine what is the ultimate noise limit both theoretically, and in real time holographic experiments. We will see that, in the theoretical ideal case, the limiting noise is the Shot Noise on the holographic reference beam. In reference to heterodyne detection, the reference beam is also called Local Oscillator. We will see that the ultimate theoretical limiting noise can be reached in real time holographic experiment, by using heterodyne holography [10] in off-axis configuration. This combination makes possible to fully filter off the technical noise, whose main origin is the LO beam technical noise, opening the way to holography with ultimate sensitivity [21, 22].

2 Theoretical noise

To discuss on noise in digital digital holography, we will consider both the case of off-axis holography, where the hologram is obtained from one frame of the CCD camera, and the case of phase shifting holography, where the holographic information is extracted from a sequence of M frames.

We will thus consider a sequence of M frames: I_0 to I_{M-1} (where $M = 1$ in the one shot, off axis case). For each frame I_k, let us note $I_{k,p,q}$ the CCD camera signal on each pixel, where k is the frame index, and p,q the pixel indexes along the x and y directions. The CCD signal $I_{k,p,q}$ is measured in Digital Counts (DC) units. In the typical case of the 12 bit digital camera used in experiments below, we have $0 \leq I_{k,p,q} < 4096$. For each frame k, the optical signal is integrated by over the acquisition time $T = 1/f_{\text{ccd}}$ of the CCD camera. The pixel signal $I_{k,p,q}$ is thus defined by :

$$I_{k,p,q} = \int_{t_k - T/2}^{t_k + T/2} dt \iint_{(p,q)} dxdy \ |E(x,y,t) + E_{LO}(x,y,t)|^2 \tag{1}$$

where $\iint_{(p,q)} dxdy$ represents the integral over the pixel (p,q) area, and where t_k is the recording moment of frame k. Introducing the complex representations $\mathscr{E}$ and $\mathscr{E}_{LO}$ of the fields E and E_{LO}, we get :

$$E(x,y,t) = \mathscr{E}(x,y)e^{j\omega_I t} + c.c. \tag{2}$$

$$E_{LO}(x,y,t) = \mathscr{E}_{LO}(x,y)e^{j\omega_{LO} t} + c.c \tag{3}$$

$$I_{k,p,q} = a^2 T \left(|\mathscr{E}_{p,q}|^2 + |\mathscr{E}_{LO}|^2 + \mathscr{E}_{p,q}\mathscr{E}_{LO}^* \cdot e^{(j(\omega_I - \omega_{LO})t_k)} + c.c. \right) \tag{4}$$

where a is the pixel size. To simplify the notations in Eq.4, we have considered that the LO field $\mathscr{E}_{LO}$ is the same in all locations (x,y), and that signal field $\mathscr{E}_{p,q}$ does not vary within the pixel (p,q). If $\mathscr{E}_{LO}$ varies with location, one has to replace $\mathscr{E}_{LO}$ by $\mathscr{E}_{LO,p,q}$ in Eq.4.

In the single-shot, off-axis holography case, the hologram H is simply $H \equiv I_k$. In order to simplify the discussion in the phase shifting digital holography case [9], we will consider 4 phases holographic detection ($M = 4n$). In that case, the phase shift of the LO beam equal to $\pi/2$ from one recorded frame to the next. Because of this shift, the complex hologram H is obtained by summing the sequence of M frames I_1 to I_M with the appropriate phase coefficient :

$$H \equiv \sum_{k=1}^{M} (j)^{k-1} I_k \tag{5}$$

where H is a matrix of pixel $H_{p,q}$, and where $M = 4n$ in the 4-phases phase-shifting case, and $M = 1$ in the single-shot, off-axis case. We get from Eq.4 :

$$H_{p,q} = \sum_{k=1}^{M} (j)^k I_{k,p,q} = 4na^2 T \mathscr{E}_{p,q} \mathscr{E}^*_{LO} \tag{6}$$

The complex hologram $H_{p,q}$ is thus proportional to the object field $\mathscr{E}_{p,q}$ with a proportionality factor that involves $\mathscr{E}^*_{LO}$.

2.1 The Shot Noise on the CCD pixel signal

Because of spontaneous emission, laser emission and photodetection are random processes, the signal that is obtained on a CCD pixel exhibits a Poisson noise called "shot noise". The effect of this Poisson noise on the signal, and on the holographic images, is the Ultimate Theoretical Limiting noise, which we will study here.

We can split the signal $I_{k,p,q}$: we get for frame k and pixel (p,q), in a noiseless average component $\langle I_{k,p,q} \rangle$ (here $\langle\ \rangle$ is the statistical average operator) and a noise component $i_{k,p,q}$:

$$I_{k,p,q} \equiv \langle I_{k,p,q} \rangle + i_{k,p,q} \tag{7}$$

To go further in the discussion, we will use photo electrons Units to measure the signal $I_{k,p,q}$.

We must notice that the local oscillator signal $\mathscr{E}_{LO}$ is large, and corresponds to a large number of photo electrons (e). In real life, this assumption is true. For example, if we adjust the power of the LO beam to be at the half maximum for the camera signal in DC unit (2048 DC for a 12 bits camera), the pixel signal will be about 10^4 e for the camera used below in experiments, since the "Camera Gain" is 4.8 e per DC. This yields two consequences, which simplify the analysis. First, the signal $I_{k,p,q}$ exhibits a gaussian distribution around its statistical average. Second, both the quantization noise of the photo electron signal ($I_{k,p,q}$ is an integer in photo electron Units), and the quantization noise of the Digital Count signal ($I_{k,p,q}$ is an integer in DC Units) can be neglected. These approximations are valid, since the width of the $I_{k,p,q}$ gaussian distribution is much larger than one in both photo electron and DC Units. In the example given above, $\langle I_{k,p,q} \rangle \simeq 10^4$, and this width is $\simeq 10^2$ in photo electron Units, and $\simeq 20$ in DC Units. One can thus consider that $I_{k,p,q}$, $\langle I_{k,p,q} \rangle$ and $i_{k,p,q}$ are floating numbers (and not integer). Moreover, $i_{k,p,q}$ is a random Gaussian distribution, with :

$$\langle i_{k,p,q} \rangle = 0 \tag{8}$$

$$\langle i^2_{k,p,q} \rangle = \langle I_{k,p,q} \rangle \tag{9}$$

To analyse the shot noise's contribution to the holographic signal $H_{p,q}$, one of the most simple method is to perform Monte Carlo simulation from Eq.7, Eq.8 and Eq.9. Since $I_{k,p,q}$ is ever large in real life (about 10^4 in our experiment), $\langle I_{k,p,q} \rangle$ can be replaced by $I_{k,p,q}$ (which is measured in experiment) in the right member of Eq.9. One has thus:

$$\langle i^2_{k,p,q} \rangle = \langle I_{k,p,q} \rangle \simeq I_{k,p,q} \tag{10}$$

Monte Carlo simulation of the noise can be done from Eq.7, Eq.8 and Eq.10

2.2 The Object field Equivalent Noise for 1 frame

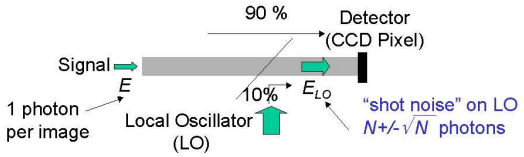

Fig. 1 1 photon equivalent signal (accounting Heterodyne gain), and shot noise on the holographic Local Oscillator beam.

In order to discuss the effect of the shot noise on the heterodyne signal $\mathscr{E}_{p,q}\mathscr{E}^*_{LO}$ of Eq.4, let us consider the simple situation sketched on Fig.1. A weak object field E, with 1 photon or 1 photo electron per pixel and per frame, interferes with a LO field E_{LO} with N photons, where N is large ($N = 10^4$, in the case of our experiment). Since the LO beam signal $a^2T|\mathscr{E}_{LO}|^2$ is equal to N photons, and the object field signal $a^2T|\mathscr{E}_{p,q}|^2$ is one photon, we have:

$$I_{k,p,q} = N + 1 + i_{k,p,q} + a^2T\mathscr{E}_{p,q}\mathscr{E}^*_{LO}e^{\cdots} + c.c. \tag{11}$$

The heterodyne signal $\mathscr{E}_{p,q}\mathscr{E}^*_{LO}$ is much larger than $|\mathscr{E}_{p,q}|^2$. This is the gain effect, associated to the coherent detection of the field $\mathscr{E}_{p,q}$. This gain is commonly called "heterodyne gain", and is proportional to the amplitude of the LO field $\mathscr{E}^*_{LO}$.

The purpose of the present discussion is to determine the effect of the noise term $i_{k,p,q}$ in Eq.11 on the holographic signal $H_{p,q}$. Since $H_{p,q}$ involves only the heterodyne term $\mathscr{E}_{p,q}\mathscr{E}^*_{LO}$ (see Eq.6), we have to compare, in Eq.11, the shot noise term $i_{k,p,q}$, and the heterodyne term $\mathscr{E}_{p,q}\mathscr{E}^*_{LO}$.

Consider first the shot noise term. We have

$$\langle i^2_{k,p,q}\rangle = \langle I_{k,p,q}\rangle = N + 1 \simeq N \tag{12}$$

The variance of the shot noise term is thus $N^{1/2}$. Since this noise is mainly related to the shot noise on the local oscillator (since $N \gg 1$), one can group together, in Eq.11, the LO beam term (i.e. N) with the noise term $i_{k,p,q}$, and consider that the LO beam signal fluctuates, the number of LO beam photons being thus "$N \pm N^{1/2}$", as mentioned on Fig.1.

Consider now the the heterodyne beat signal. Since we have N photons on the LO beam, and 1 photon on the object beam, we get:

$$a^2T|\mathscr{E}_{p,q}\mathscr{E}^*_{LO}| \equiv \left(\left(a^2T|\mathscr{E}_{p,q}|^2\right)\left(a^2T|\mathscr{E}_{LO}|^2\right)\right)^{1/2} = N^{1/2} \tag{13}$$

The heterodyne beat signal $\mathscr{E}_{p,q}\mathscr{E}^*_{LO}$ is thus $N^{1/2} = 100$.

The shot noise term $i_{k,p,q}$ is thus equal to the heterodyne signal $\mathscr{E}_{p,q}\mathscr{E}_{LO}^{*}$ corresponding to 1 photon on the object field. This means that shot noise $i_{k,p,q}$ yields an equivalent noise of 1 photon per pixel, on the object beam. This result is obtained here for 1 frame. We will show that it remains true for a sequence of M frames, whatever $M = 4n$ is.

2.3 The Object field Equivalent Noise for $M = 4n$ frames

Let us introduce the DC component signal D, which is similar to the heterodyne signal H given by Eq.5, but without phase factors:

$$D \equiv \sum_{k=1}^{M} I_k \tag{14}$$

The component D can be defined for each pixel (p,q) by :

$$D_{p,q} \equiv \sum_{k=1}^{M} I_{k,p,q} \tag{15}$$

Since $I_{k,p,q}$ is always large in real life (about 10^4 in our experiment), the shot noise term can be neglected in the calculation of $D_{p,q}$ by Eq.15. We have thus:

$$D_{p,q} \equiv \sum_{k=1}^{M} I_{k,p,q} = Ma^2T\left(|\mathscr{E}_{p,q}|^2 + |\mathscr{E}_{LO}|^2\right) \tag{16}$$

We are implicitly interested by the low signal situation (i.e. $\mathscr{E}_{p,q} \ll \mathscr{E}_{LO}$) because we focus on noise analysis. In that case, the $|\mathscr{E}_{p,q}|^2$ term can be neglected in Eq.16. This means that $D_{p,q}$ gives a good approximation for the LO signal.

$$D_{p,q} \equiv \sum_{k=1}^{M} I_{k,p,q} \simeq Ma^2T|\mathscr{E}_{LO}|^2 \tag{17}$$

We can get then the signal field $|\mathscr{E}_{p,q}|^2$ from Eq.6 and Eq.17:

$$\frac{|H_{p,q}|^2}{D_{p,q}} \simeq Ma^2T|\mathscr{E}_{p,q}|^2 \tag{18}$$

In this equation, the ratio $|H_{p,q}|^2/D_{p,q}$ is proportional to the number of frames of the sequence ($M = 4n$), This means that $|H_{p,q}|^2/D_{p,q}$ represents the signal field $|\mathscr{E}_{p,q}|^2$ summed over the all frames.

Let us calculate the effect of the shot noise on $|H_{p,q}|^2/D_{p,q}$. To calculate this effect, one can make a Monte Carlo simulation as mentioned above, but a simpler calculation can be done here. Let us develop $|H_{p,q}|$ in statistical average and noise

components (as done for $I_{k,p,q}$ in Eq.7):

$$H_{p,q} = \langle H_{p,q} \rangle + h_{p,q} \tag{19}$$

with

$$h_{p,q} = \sum_{k=1}^{4n} j^{\,k} i_{k,p,q} \tag{20}$$

Let us calculate $\langle |H_{p,q}|^2 / D_{p,q} \rangle$ from Eq.18. Since $D_{p,q} \simeq \langle D_{p,q} \rangle$, we get :

$$\left\langle \frac{|H_{p,q}|^2}{D_{p,q}} \right\rangle \simeq \frac{|\langle H_{p,q} \rangle|^2 + \langle |h_{p,q}|^2 \rangle + \langle \langle H_{p,q} \rangle h^*_{p,q} \rangle + \langle \langle H^*_{p,q} \rangle h_{p,q} \rangle}{\langle D_{p,q} \rangle} \tag{21}$$

In Eq.21 the $\langle \langle H_{p,q} \rangle h^*_{p,q} \rangle$ term is zero since $h^*_{p,q}$ is random while $\langle H_{p,q} \rangle$ is not. The two terms $\langle \langle H_{p,q} \rangle h^*_{p,q} \rangle$ and $\langle \langle H^*_{p,q} \rangle h_{p,q} \rangle$ can be thus removed. On the other hand, we get for $|h_{p,q}|^2$

$$|h_{p,q}|^2 = \sum_{k=1}^{4n} |i_{k,p,q}|^2 + \sum_{k=1}^{4n} \sum_{k'=1, k' \neq k}^{4n} j^{\,k-k'} i_{k,p,q} i_{k',p,q} \tag{22}$$

Since $i_{k,p,q}$ and $i_{k',p,q}$ are uncorrelated, the $i_{k,p,q} i_{k',p,q}$ terms cancel in the calculation of the statistical average of $|h_{p,q}|^2$. We get then from Eq.9

$$\langle |h_{p,q}|^2 \rangle = \sum_{k=1}^{4n} \langle |i_{k,p,q}|^2 \rangle = \sum_{k=1}^{4n} \langle I_{k,p,q} \rangle = \langle D_{p,q} \rangle \tag{23}$$

Eq.21 becomes thus :

$$\left\langle \frac{|H_{p,q}|^2}{D_{p,q}} \right\rangle = \frac{|\langle H_{p,q} \rangle|^2}{\langle D_{p,q} \rangle} + 1 \tag{24}$$

Equation 24 means that the average detected intensity signal $\langle |H_{p,q}|^2 / D_{p,q} \rangle$ is the sum of the square of the average object field $\langle |H_{p,q}| \rangle / (\langle D_{p,q} \rangle^{1/2})$ plus one photo-electron. Without illumination of the object, the average object field is zero, and the detected signal is 1 photo-electron. The equation establishes thus that the LO shot noise yields a signal intensity corresponding exactly to 1 photo-electron (e) per pixel.

The 1 e noise floor, we get here, can be also interpreted as resulting from the heterodyne detection of the vacuum field fluctuations [23].

3 Reaching the Shot Noise in real life holographic experiment.

In section 2, we have shown that the theoretical noise on the holographic reconstructed intensity images is 1 photo electron per pixel whatever the number of

recorded frames is. We will now discuss the ability to reach this limit in real time holographic experiment. Since we consider implicitly a very weak object beam signal ($\mathscr{E} \ll \mathscr{E}_{LO}$), the noises that must be considered are the readout noise of the CCD camera, the technical noise from laser amplitude fluctuations on the LO beam, and the LO beam shot noise, which yields the theoretical noise limit.

Consider a typical holographic experiment made with a PCO Pixelfly 12 bit digital camera. The LO beam power is adjusted in order to be at half saturation of the digital camera output. Since the camera is 12 bits, and since the camera "gain" is 4.8e/DC, half saturation corresponds to 2000 DC on the A/D Converter, i.e. about 10^4 e on the each CCD pixel . The LO shot noise, which is about 100 e, is thus much larger than the Pixelfly Read Noise (20 e), Dark Noise (3 e/sec) and A/D quantization noise (4.8 e, since 1 DC corresponds to 4.8 e). The noise of the camera can be neglected, and is not a limiting factor for reaching the noise theoretical limit.

The LO beam that reaches the camera is essentially flat field (i.e. the field intensity $|\mathscr{E}_{LO}|^2$ is roughly the same for all the pixels). The LO beam technical noise is thus highly correlated in all pixels. This is in particular the case for the noise induced by the fluctuations of the main laser intensity, or by the vibrations of the mirrors within the LO beam arm. To illustrate this point, we have recorded a sequence of $M = 4n = 4$ frames I_k (with $k = 0...3$) with a LO beam, but without signal from the object (i.e. without illumination of the object). We have thus recorded the hologram of the "vacuum field". We have calculated then the complex hologram $H(x,y)$ by Eq.5, and the reciprocal space hologram $\tilde{H}(k_x,k_y)$ by Fourier transform:

$$\tilde{H}(k_x,k_y) = \text{FFT}\ \ H(x,y) \tag{25}$$

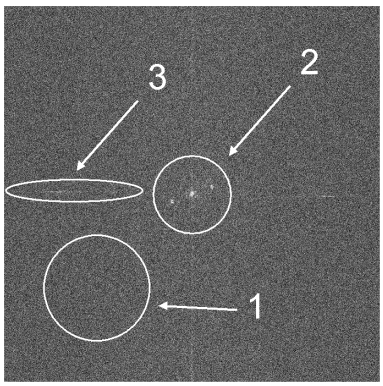

Fig. 2 Intensity image of $\tilde{H}(k_x,k_y,0)$ for $M = 4n = 4$ frames without illumination of the object (no signal field $\mathscr{E}$). Three kind of noises can be identified. Down left (1) : shot noise; center (2): technical noise of the CCD; left (3) : FFT aliasing. By truncating the image and keeping only the left down part, the shot noise limit is reached. The image is displayed in arbitrary logarithm grey scale.

The reciprocal space holographic intensity $|\tilde{H}|^2$ is displayed on Fig.2 in arbitrary logarithm grey scale. On most of the reciprocal space (within for example circle 1), $|\tilde{H}|^2$ corresponds to a random speckle whose average intensity is uniformly distributed along k_x and k_y. One observes nevertheless bright points within circle 2, which corresponds to $(k_x,k_y) \simeq (0,0)$. These points correspond to the technical

noise, which is flat field within the CCD plane (x,y), and which corresponds thus to low spatial frequency components gathered around the center of the (k_x,k_y) reciprocal space. One see also, on the Fig.2 image, an horizontal and a vertical bright line, which corresponds to $k_y \simeq 0$ and $k_x \simeq 0$ (zone 3 on Fig.2). These parasitic bright lines are related to Fast Fourier Transform aliases, that are related to the discontinuity of the signal I_k and H at edge of the calculation grid, in the (x,y) space.

We have measured $\langle|\tilde{H}|^2\rangle$ by replacing the statistical average $\langle\ \rangle$ by a spatial average over a region of the conjugate space without technical noise (i.e. over region 1). This gives a measurement of $\langle|\tilde{H}|^2\rangle$, i.e. a measurement of $\langle|H|^2\rangle$, since the space average of $|\tilde{H}|^2$ and $|H|^2$ are equal, because of the FFT Parceval theorem. We have also measured D from the sequence of frames I_k with $k = 0...3$ (see Eq.14). Knowing the camera Analog Digital (A/D) conversion factor (4.8 e/DC), we have calculated the noise intensity $\langle|\tilde{H}|^2\rangle/\langle D\rangle$ in photo-electron units, and we get, within 10%, one photo electron per pixel for the average noise within region 2, as expected theoretically for the shot noise (see Eq.21).

To verify that we have truly reached the shot noise limit, we have performed a control experiment with a camera illuminated by a tungsten lamp powered by a battery. The lamp provides here a clean white light source. The lamp voltage is adjusted to get half saturation of the camera (about 2000 DC). Like with the laser experiment described above, we have recorded a sequence of $M = 4n = 4$ frames I_k with $k = 0...3$, and we have calculated $H(x,y)$, and $\tilde{H}(k_x,k_y)$. The image of $|\tilde{H}(k_x,k_y)|^2$ we get is very similar to Fig.2. Moreover, the average noise intensity in region 2 is exactly the same as with a laser (one photo electron per pixel). One has thus :

$$\langle|\tilde{H}|^2\rangle/\langle D\rangle = 1 \tag{26}$$

This result is expected since the camera "gain" is measured by assuming that the noise obtained in clean lamp control experiment is shot noise limited [24]. Assuming Eq.26, where $\langle|\tilde{H}|^2\rangle/\langle D\rangle$ depends on the camera "gain", is thus equivalent to make a measurement of the "gain" in e/DC Units. The control experiment made here, redoes the "gain" calibration made by the camera manufacturer (i.e. PCO). We simply get here, within 10%, the same camera gain $(4.8e/\mathrm{DC})$.

3.1 Experimental validation with an USAF target.

We have verified that it is possible to perform shot noise limited holography in real life, by recording the hologram of an USAF target in transmission. The holographic setup is sketched on Fig.3. We have recorded sequences of $M = 4n = 12$ frames, and we have reconstructed the image of the USAF target.

Figure 4 shows the holographic reconstructed images of the USAF target. The intensity of the signal illumination is adjusted with neutral density filters. In order to filter-off the technical noise, the reconstruction is done by selecting the order 1 image of the object, within the reciprocal space [8]. Since the 400×400 pixels

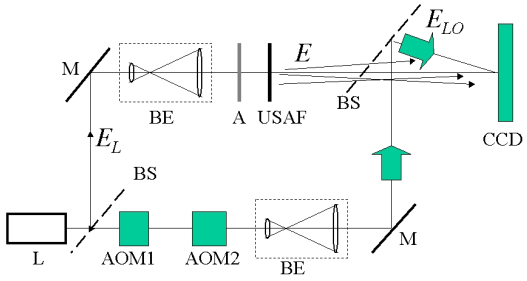

Fig. 3 Setup of the test experiment with USAF target. L: main laser; BS: Beam splitter; AOM1 and AOM2: acousto-optic modulators; BE: beam expander; M: mirror; A1 and A2: light attenuators. USAF: transmission USAF target that is imaged. CCD : CCD camera.

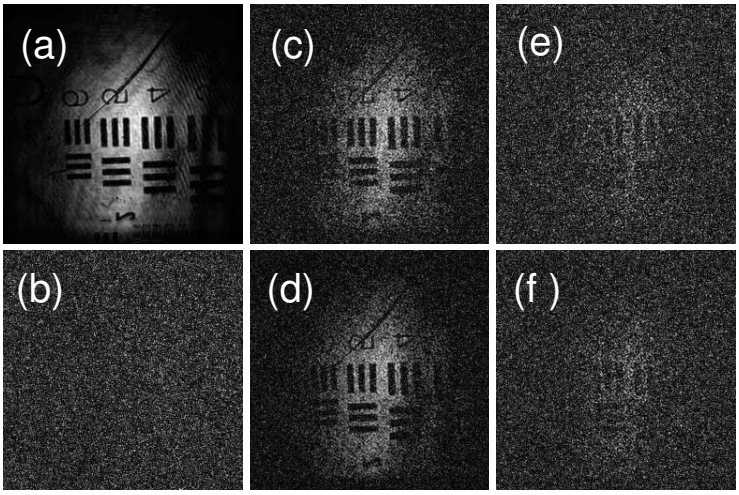

Fig. 4 (a,c,d): Reconstructions of an USAF target with different level of illumination 700 (a), 1 (c) and 0.15 e/pixel (d). (b): Simulated Shot Noise noise image. (e,f): Simulated reconstructed image obtained by mixing image (a) with weight X, and image (b) with weight $1-X$. The weight X is $1/700$ (e), and $0.15/700$ (f). Images are displayed in arbitrary logarithmic grey scale.

region that is selected is off-axis, the low spatial frequency noisy region, which correspond to the zero order contributions (region 1 on Fig.2), is filtered-off.

Figure 4 (a,c,d) shows the reconstructed images obtained for different illumination levels of the USAF target. For each image, we have measured the average number of photo electrons per pixel corresponding to the object beam, within the reciprocal space region that has been selected for the reconstruction (i.e. 400×400 pixels). The images of Fig. 4 correspond to 700 (a), 1 (c), and 0.15 (d) electron per pixel for the sequence of $M = 4n = 12$ frames respectively (i.e. $700/12$, $1/12$ and $0.15/12$ e per pixel and per frame).

Here, the object beam intensity has been measured by the following way. We have first calibrated the response of our camera with an attenuated laser whose power is known. We have then measured with the camera, at high level of signal, the intensity of the signal beam alone (without LO beam). We have decreased, to the end, the

signal beam intensity by using calibrated attenuators in order to reach the low signal level of the images of Fig. 2 (a,c,d). In the case of image (a) with 700e/pix, we also have measured the averaged signal intensity from the data themselves by calculating $|H|^2/D$ (see Eq.18). The two measurements gave the same result: 700e per pixel.

On figure 4 (a), with 700e per pixel, the USAF signal is much larger than the shot noise, and the Sinal to Noise Ratio (SNR) is large. On figure 4 (c), with 1e per pixel, the USAF signal roughly equal to the shot noise, and the SNR is about 1. With 0.15e per pixel, the SNR is low on Fig.4 (d) (about 0.15), and the USAF is hardly seen.

It is nevertheless quite difficult to evaluate the SNR of an image. To perform a more quantitative analysis of the noise within the images, we have synthesized the noisy images of Fig.4 (e,f) by adding noise to the Fig. 4 (a) noiseless image. We have first synthesized a pure Noise image, which is displayed on Fig.4 (b). The Noise image, which corresponds to the image that is expected without signal, is obtained by the following way. From one of the measured frames (for example I_0) we have calculated the noise components $i_{k,p,q}$ by Monte Carlo drawing with the condition:

$$\langle i_{k,p,q}^2 \rangle = I_{0,p,q} \tag{27}$$

This condition corresponds to Eq.9 since $\langle I_{k,p,q} \rangle \simeq I_{0,p,q}$. We have synthesized the image sequence I_k in the following manner:

$$I_{k,p,q} = I_{0,p,q} + i_{k,p,q} \tag{28}$$

The Shot Noise image of Fig.4 (b) is reconstructed then from the $I_{k,p,q}$ sequence with $k = 0...12$ since $M = 4n = 12$.

We have synthesized noisy images by summing the noiseless image of Fig.4 (a) with weight X, with the Noise image of Fig.4 (b) with weight $(1-X)$. The image of Fig. 4 (e) is obtained with $X = 1/700$. Figure 4 (e) corresponds thus to the same signal, and the same noise than Figure 4 (c) (i.e. 1e of signal, and 1e of noise respectively). As expected, Fig. 4 (c) and Fig. 4 (e) are visually very similar. The image of Fig. 4 is similarly obtained with $X = 0.15/700$. It corresponds to the same Signal and Noise than Figure 4 (d) (i.e. 0.15e of signal, and 1e of noise). As expected, Fig. 4 (d) and Fig. 4 (f) are visually very similar too.

Here we demonstrated our ability to synthesize a noisy image with a noise that is calculated by Monte Carlo from Eq.27 and 28. Moreover, we have verified that the noisy image is visually equivalent to the image we have obtained in experiments. These results prove that we are able to assess quantitatively the noise, and that the noise that is obtained in experiments reaches the theoretical limit of 1e of noise per pixel for the whole sequence of $M = 4n = 12$ frames.

4 Conclusion

In this paper we have studied the noise limits in off-axis, heterodyne digital holography. We have shown that because of the heterodyne gain of the holographic de-

tection, the noise of the CCD camera can be neglected. Moreover by a proper arrangement of the holographic setup, that combines off-axis geometry with phase shifting acquisition of holograms by heterodyne holography, it is possible to reach the theoretical shot noise limit. We have studied theoretically this limit, and we have shown that it corresponds to 1 photo electron per pixel for the whole sequence of frame that is used to reconstruct the holographic image. This paradoxical result is related to the heterodyne detection, where the detection bandwidth is inversely proportional to the measurement time. We have verified all our results experimentally, and we have shown that is possible to image objects at very low signal levels. We have also shown that is possible to mimic the very weak illumination levels holograms obtained in experiments by Monte Carlo noise modeling.

References

1. D. Gabor. Microscopy by reconstructed wavefronts. *Proc. R. Soc. A*, 197:454, 1949.
2. A. Macovsky. Consideration of television holography. *Optica Acta*, 22(16):1268, August 1971.
3. U. Schnars. Direct phase determination in hologram interferometry with use of digitally recorded holograms. *JOSA A.*, 11:977, July 1994.
4. J. W. Goodmann and R. W. Lawrence. Digital image formation from electronically detected holograms. *Appl. Phys. Lett.*, 11:77, 1967.
5. E.N. Leith, J. Upatnieks, and K.A. Haines. Microscopy by wavefront reconstruction. *Journal of the Optical Society of America*, 55(8):981–986, 1965.
6. U. Schnars and W. Jüptner. Direct recording of holograms by a CCD target and numerical reconstruction. *Appl. Opt.*, 33(2):179–181, 1994.
7. T. M. Kreis, W. P. O. Juptner, and J. Geldmacher. Principles of digital holographic interferometry. *SPIE*, 3478:45, July 1988.
8. Etienne Cuche, Pierre Marquet, and Christian Depeursinge. spatial filtering for zero-order and twin-image elimination in digital off-axis holography. *Appl. Opt.*, 39(23):4070–4075, 2000.
9. I. Yamaguchi and T. Zhang. Phase-shifting digital holography. *Optics Letters*, 18(1):31, 1997.
10. F. LeClerc, L. Collot, and M. Gross. Numerical heterodyne holography using 2d photodetector arrays. *Optics Letters*, 25:716, Mai 2000.
11. M. Atlan, M. Gross, and E. Absil. Accurate phase-shifting digital interferometry. *Optics letters*, 32(11):1456–1458, 2007.
12. M. Gross, P. Goy, and M. Al-Koussa. Shot-noise detection of ultrasound-tagged photons in ultrasound-modulated optical imaging. *Optics letters*, 28(24):2482–2484, 2003.
13. M. Atlan, BC Forget, F. Ramaz, AC Boccara, and M. Gross. Pulsed acousto-optic imaging in dynamic scattering media with heterodyne parallel speckle detection. *Optics letters*, 30(11):1360–1362, 2005.
14. L. Wang and X. Zhao. Ultrasound-modulated optical tomography of absorbing objects buried in dense tissue-simulating turbid media. *Applied optics*, 36(28):7277–7282, 1997.
15. F. Joud, F. Laloe, M. Atlan, J. Hare, and M. Gross. Imaging a vibrating object by Sideband Digital Holography. *Optics Express*, 17:2774, 2009.
16. F. Joud, F. Verpillat, F. Laloë, M. Atlan, J. Hare, and M. Gross. Fringe-free holographic measurements of large-amplitude vibrations. *Optics Letters*, 34(23):3698–3700, 2009.
17. M. Atlan, M. Gross, and J. Leng. Laser Doppler imaging of microflow. *J. Eur. Opt. Soc. Rapid Publications*, 1:06025–1, 2006.
18. M. Atlan, M. Gross, BC Forget, T. Vitalis, A. Rancillac, and AK Dunn. Frequency-domain wide-field laser Doppler in vivo imaging. *Optics letters*, 31(18):2762–2764, 2006.

19. M. Atlan, B.C. Forget, A.C. Boccara, T. Vitalis, A. Rancillac, A.K. Dunn, and M. Gross. Cortical blood flow assessment with frequency-domain laser Doppler microscopy. *Journal of Biomedical Optics*, 12:024019, 2007.
20. M. Atlan, M. Gross, T. Vitalis, A. Rancillac, J. Rossier, and AC Boccara. High-speed wave-mixing laser Doppler imaging in vivo. *Optics Letters*, 33(8):842–844, 2008.
21. M. Gross and M. Atlan. Digital holography with ultimate sensitivity. *Optics Letters*, 32(8):909–911, 2007.
22. M. Gross, M. Atlan, and E. Absil. Noise and aliases in off-axis and phase-shifting holography. *Applied Optics*, 47(11):1757–1766, 2008.
23. H.A. Bachor, T.C. Ralph, S. Lucia, and T.C. Ralph. *A guide to experiments in quantum optics*. wiley-vch, 1998.
24. M. Newberry. Measuring the Gain of a CCD Camera. *Axiom Technical Note: 1*, 1:1–9, 1998-2000.